Characterization of Upper-limb Pathological Tremors: Application to Design of an Augmented Haptic Rehabilitation System*

S. Farokh Atashzar, *Student Member, IEEE*, Mahya Shahbazi, *Student Member, IEEE*, Olivia Samotus, Mahdi Tavakoli, *Member, IEEE*, Mandar Jog, *MD*, Rajni V. Patel, *Life Fellow, IEEE*

Abstract—In this paper, an adaptive filtering technique is proposed to estimate and characterize pathological tremors caused by Parkinson's disease (PD) and Essential Tremor (ET). The technique is based on the formulation of Band-limited Multiple Fourier Linear Combiners (BMFLC) and is called Enhanced-BMFLC (E-BMFLC). The effectiveness of the designed filter is statistically evaluated through a clinical study involving 14 PD and 13 ET patients. The hand tremors of the participants are studied in three Degrees of Freedom (DOF). Using statistical analysis, it is shown that the new design of the filter significantly enhances the accuracy in comparison with the performance of conventional BMFLC filtering. In addition, E-BMFLC significantly reduces the sensitivity to parameter tuning and intra-patient variabilities. The observed improvements are achieved by modulating the memory of the proposed filter, and by enriching the utilized harmonic model. The proposed filter is then used to develop a safe haptics-enabled robotic rehabilitation architecture, designed for patients having hand tremors. The architecture is entitled Augmented Haptic Rehabilitation (AHR) which enables adaptive management of the involuntary components of the hand motion while delivering assist-as-needed haptic therapy (for the voluntary component) and avoiding unsafe amplification of hand tremors. Experimental evaluations are provided to evaluate the efficacy of the proposed AHR system.

Index Terms—Adaptive Filters, Pathological Hand Tremors, Assist-as-needed Robotic Rehabilitation.

List of Acronyms

FLC: Fourier Linear Combiner, **WFLC:** Weighted-frequency FLC, **BMFLC:** Band-limited Multiple FLC, **E-BMFLC:** Enhanced-BMFLC, **AHR:** Augmented Haptic Rehabilitation, **NP:** Neuro-Plasticity, **OTP:** Old Tremor Projection, **HRR:** Haptics-enabled Robotic Rehabilitation, **PVT:** Programmable Virtual Therapist, **PD:** Parkinson's Disease, **ET:** Essential Tremor, **TA:** Tremor Amplification.

I. Introduction and Preliminaries

Based on official statistics, the population of adults over the age of 65 is rapidly increasing worldwide. This trend is anticipated to continue due to the increase in life expectancy, and reduced fertility rate. It is anticipated that the number of senior adults will be more than twice by 2050 compared to the corresponding number in 2013 [1]. As a result of this ageing society, it is expected that there will be a significant increase in the incidence rate of age-related sensorimotor disorders and diseases such as Parkinson's Disease (PD) and Essential Tremor (ET). PD and ET are known to affect coordination, targeting and speed of motion while causing involuntary hand tremor [2], [3], [4]. Processing of hand motion and real-time extraction of the involuntary components while introducing minimum lag is an active line of research. This has attracted a great deal of interest for designing assistive, wearable and rehabilitative technologies by utilizing kinesthetic inputs and electrical stimulations (see, e.g., [5], [6], [7], [8], [9]).

Adaptive filters developed based on a Fourier Linear Combiner (FLC) algorithm have demonstrated appropriate performance in extracting hand tremors while introducing minimum latency compared to classical filtering [10], [11], [12], [13], [14], [15]. The original version of recursive FLC-based filters, i.e., Weighted-frequency Fourier Linear Combiner (WFLC), was developed based on the assumption of having a single dominant frequency [10] for the targeted signals. The filter was used to design hand-held surgical tools in order to cancel physiological tremor of surgeons' hands, in real-time (a practical need for delicate microsurgery) [11]. The assumption of a single dominant frequency was relaxed by proposing the BMFLC technique which can track multiple harmonics of a signal. The original motivation was to extract physiological hand tremor in healthy subjects [12], [13], [14]. The BMFLC filter has been utilized to extract physiological hand tremor [16] for surgical applications [17], [18] and its performance has been compared with that of the WFLC filter in quantification of hand tremors of microsurgeons and considerable improvement has been reported [13]. Due to appropriate performance of BMFLC filters in extracting physiological tremors, a recent study has investigated the possibility of using the technique for pathological hand tremors (such as those in PD) [15]. For this purpose, in [15], a new modification of the BMFLC filter was proposed to find the dominant frequency of the signal. Although the per-

formance of the technique in [15] was slightly inferior to that of the conventional BMFLC filter, it was able to automatically find the dominant frequency of interest.

It should be noted that there are distinct differences between pathological and physiological tremors in terms of (a) amplitude, (b) frequency content, and (c) variability. In contrast to physiological tremors, pathological involuntary movements caused by PD and ET have closer range of frequencies to voluntary actions. However, for physiological hand tremor, the frequency range of involuntary movements is considerably higher than that for voluntary components of the motion. This makes it possible to deal with the voluntary components of motion through the use of a bias term in the model for the case of physiological tremor [12], [13]. The close frequency range of pathological hand tremors to the voluntary components can challenge the estimation problem using various filtering techniques, specially in real-time applications. In addition to the frequency range, the nature, amplitude and existence of the tremor is considerably variable for the case of pathological tremors and they change considerably during task performance. Characteristics of pathological tremors in PD and ET patients depend on position, velocity, posture, task, and loading conditions. As an example, in Fig. 1, the hand tremor of a patient (participant #23 in our study, a 84 years old male with ET) is demonstrated for the cases of no-load posturing (Fig. 1(a)) and with-load posturing (Fig. 1(b)). In this test, the patient is asked to keep the posture steady while holding a cup under two loading conditions (i.e. empty cup and 1-pound loaded cup). Each loading condition is performed for 10 seconds. We overlaid 10 snapshots of each condition during the corresponding period of the test to produce Figs. 1(a) and 1(b). In addition, the results of measuring the hand accelerations in 3 DOF are given in Fig. 1(c). As can be seen, there is almost no tremor during no-load posturing for this participant while high-amplitude tremors start right after adding the 1-pound weight to the cup. This is just one example of how variable the pathological tremors can be under different conditions.

The BMFLC filters were designed originally for physiological tremors. Consequently, using them for pathological hand tremors should be statistically studied. For example, since there are considerable variations in the nature of hand tremors for each patient in different posturing, motion and load conditions, the filter needs to have low sensitivity to parameter tuning. In other words, when we tune the main parameter of the BMFLC filter (which is a corrective gain, defined later in this paper), we need to be confident that the filter will keep good performance during the task, even if the type and nature of a hand tremor changes. It will not be practical if the filter is sensitive to the tuning of the corrective gain. The reason is that in this case, for each part of the task (which may require a different load or posturing condition) the filter may need a different corrective gain to deliver appropriate performance. This is not practical.

Consequently, although the use of the BMFLC filter is promising for extracting pathological tremors, the performance of this filter needs to be statistically analyzed for
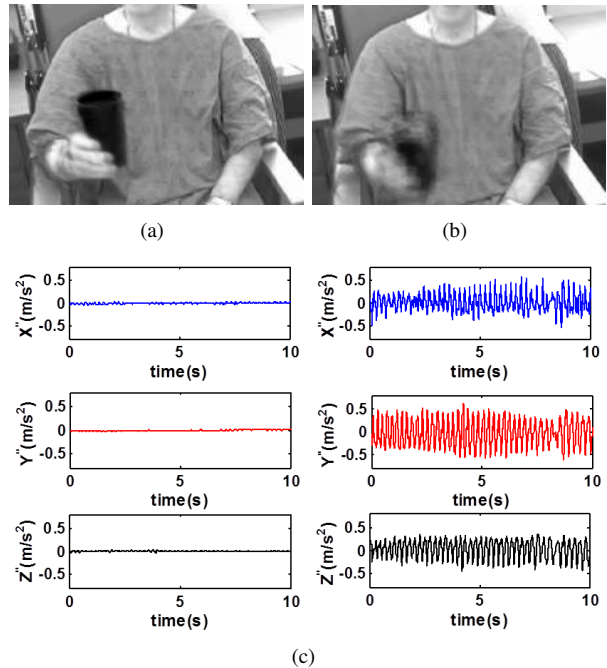

Fig. 1. Participant #23 Holding the cup while maintaining a posture: (a) overlaid 10 snapshots during 10 seconds for the case of an empty cup, (b) overlaid 10 snapshots during 10 seconds for the case of a loaded cup, (c) hand accelerations in X-direction (solid blue line), Y-direction (solid red line), and Z-direction (solid black line) for the case of the empty cup experiment (left) and the loaded cup experiment (right). In (b), the blurred image of the patient's hand is due to high amplitude tremor.

a group of pathological patients and the possibility of enhancing performance should be evaluated to be compatible with the characteristics of pathological tremors.

A. Focus of This Paper

Motivated by the above issues, in this paper we propose a new two-step modification to make the filter more accurate in extracting tremors and less sensitive to parameter tuning and intra-patient variabilities. The two-step modifications are (a) modulating the filter's memory, and (b) enriching the harmonic model for extracting the hand tremor. The filter proposed in this paper is called "E-BMFLC".

In the next step, we conducted a clinical study including 14 PD and 13 ET patients to evaluate the efficacy of the proposed filter in comparison with the conventional BMFLC technique. Using statistical analysis, we showed that E-BMFLC not only significantly enhances the accuracy of the proposed filter, but it also substantially reduces the sensitivity to the design of the filter's parameters and intra-patient variabilities. To the best knowledge of the authors, this is the first paper showing how to improve the performance of BMFLC filters in a statistically-significant manner for patients living with pathological hand tremors.

In the second part of this study, we investigate the possibility of using the proposed E-BMFLC filter to develop a new Haptics-enabled Robotic Rehabilitation (HRR) architecture which is capable of delivering energetically-active assist-as-needed therapy for PD and ET patients while adaptively controlling their hand tremor and avoiding unsafe Tremor Amplification (TA). TA is a restrictive factor

when using non-passive robotic systems (that elevate the energy of the human-robot interaction) for patients having hand tremors. Active HRR systems amplify the energy provided by the patient and reflect it back to him/her to enhance coordination and movement speed. However, when the patient has involuntary hand tremor, elevating the total energy of the patient's hand is equal to elevating the energy of the hand tremor. This can result in an unsafe unwanted condition (i.e. TA). TA can simply degrade the performance and usability of HRR systems for patients living with hand tremor. In the literature, the use of HRR systems in patients living with hand tremors are mostly limited to assessment and analysis of the disease and not multi-modal interactive rehabilitation and intelligent exercises [19], [20], [21].

In order to address the aforementioned challenge, we propose Augmented Haptic Rehabilitation (AHR) architecture. AHR is motivated by new evidence showing that interactive Virtual Reality (VR)-based rehabilitation can considerably accelerate Neuro-Plasticity (NP) and enhance sensorimotor health and targeting accuracy for patients living with pathological tremors, such as PD [22], [23], [24], [25] and ET [26], [27], [28]. The initial concept of the architecture was briefly presented by the authors in the conference paper [29]. The AHR system presented in the current paper is an adaptive dual-action augmented haptic platform *designed based on monitoring the energy of the voluntary and involuntary components of motion*. The proposed architecture provides an adaptive viscous environment (resistive therapy) in parts of the *frequency spectrum* of the patient's motion to resist (not counteract) the hand tremor up to a point that it reaches a minimum energy level. This action of the AHR system is like an adaptive energy cap which gradually forces the energy of the patient's hand tremor to converge to a small under-control value. This action avoids TA and makes the HRR system compatible for use for tremor patients. At the same time, the AHR system provides assistive action for the voluntary component of the motion. The energy of the voluntary component and tracking error is also monitored. The assistive force field enables the patient to have an acceptable tracking performance based on the monitored energy of the voluntary movement. The intensity of the assistive therapy is adaptively and gradually tuned in a new energy-based assist-as-needed manner to provide the patient with minimum needed assistance while keeping the patient in the loop of interaction. Consequently, the proposed dual-action behavior of the AHR system allows for delivering assistance to the voluntary component of the motion while restricting the involuntary component of motion in order to avoid potential TA. This is achieved taking advantage of the accurate decomposition of the voluntary and the involuntary components of the patient's motion using the proposed E-BMFLC filter. This motion processing is the heart of the proposed AHR architecture which makes it possible to use interactive multi-modal environment of assistive HRR systems for rehabilitating slowness, coordination deficits and motion range problems (typical symptoms in PD and ET patients), in a safe manner. Fig. 2 shows the proposed
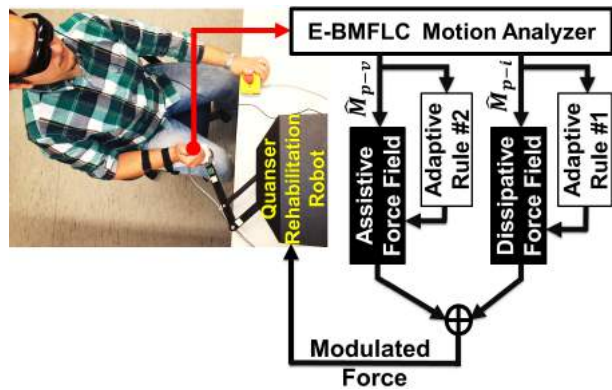

Fig. 2. Block-diagram of the designed AHR system.

AHR architecture. The architecture is implemented in this paper and experimental evaluations are reported.

Remark 1. The contributions of this paper are summarized below:

a: Showing two issues with the conventional design of BMFLC filters which can reduce the quality of the results for pathological tremor estimation, namely: infinite memory and old tremor projection.

b: Proposing two new solutions to significantly enhance the accuracy of the filter, reduce the sensitivity to parameter tuning and variation in the frequency content of the signal, and deal with the two issues mentioned above.

c: Statistically analyzing the performance of the proposed E-BMFLC filter for 27 pathological tremor patients in order to validate the functionality of the proposed technique.

d: Proposing a new AHR technique which enables delivery of a new assist-as-needed rehabilitation therapy for PD and ET patients while controlling the energy of involuntary movements and avoiding unsafe amplification of hand tremors due to the active nature of robotic therapy.

e: Experimental evaluation of the functionality of the proposed AHR system.●

The rest of this paper is organized as follows: The conventional BMFLC filter is introduced in Section II. The new E-BMFLC filter is proposed in Section III. In Section IV, the developed AHR architecture is defined. The statistical results of the clinical study on the performance of the E-BMFLC filter are given in Section V. The AHR architecture is evaluated and experimental results are reported in Section VI. Concluding remarks are given in Section VII.

II. CONVENTIONAL ADAPTIVE BMFLC FILTERING

In this section a quick overview of the conventional BMFLC filter is given, based on [12], [13], [14]. It is known that hand movement of patients living with pathological tremor is a modulated signal which has low-frequency voluntary actions and high-frequency involuntary components [6]. Accordingly, the hand motion can be modelled as:

$$M_p(t) = M_{p-v}(t) + M_{p-i}(t) \qquad (1)$$

In (1), $M_p(t)$ is a signal which corresponds to the motion of the patient's hand that can be the hand position $P_p(t)$, velocity $V_p(t)$, or acceleration $A_p(t)$. Accordingly, $M_{p-v}(t)$ is the voluntary component of the hand motion and $M_{p-i}(t)$ is the involuntary component. The main goal of the BMFLC filtering is to find an estimate for $M_{p-i}(t)$ in a real-time manner while minimizing error and lag. The output can then be used in actuated devices such as the one used for hand-held anti-tremor surgical tools [12], [13], [14].

A BMFLC filter considers a truncated Fourier model for the frequency window $[\omega_a, \omega_b]$ of the hand tremor as:

$$Y(t) = \sum_{i=0}^{i=\beta(\omega_b-\omega_a)} \lambda_i \sin(\omega_a t + \frac{i}{\beta}t) + \vartheta_i \cos(\omega_a t + \frac{i}{\beta}t). \quad (2)$$

In (2), $Y(t)$ is the signal to be modeled, ω_a and ω_b define the frequency window of interest (which correspond to the tremor frequency). β is the number of harmonics considered for one unit of frequency. Also, λ and ϑ are coefficients of the truncated Fourier combiner model. The linear regressors formulation of the truncated model (2) considering the band-limited frequency window for the hand tremor $[\omega_a, \omega_b]$ can be written as:

$$Y(t) = \theta^T \phi(t), \quad (3)$$

where we have:

$$\phi(t) = \Big[\sin(\omega_a t + \frac{0}{\beta}t), \ \dots \ , \sin(\omega_a t + \frac{\beta(\omega_b-\omega_a)}{\beta}t),$$
$$\cos(\omega_a t + \frac{0}{\beta}t), \ \dots \ , \cos(\omega_a t + \frac{\beta(\omega_b-\omega_a)}{\beta}t) \Big]^T, \quad (4)$$

$$\text{and } \theta = \Big[\lambda_0, \ \dots \ , \lambda_{\beta(\omega_b-\omega_a)}, \vartheta_0, \ \dots \ , \vartheta_{\beta(\omega_b-\omega_a)} \Big]^T. \quad (5)$$

The regressors model, defined in (3)-(5) is then utilized in a recursive Least Mean Squares (LMS) algorithm to estimate the tremor in real-time and track its amplitude and the frequency content. It should be highlighted that the LMS algorithm has been conventionally and recently used in the design of BMFLC filters [12], [13], [14], [15]. LMS has been also replaced with Kalman filtering in some studies [30], [16]. Although the use of Kalman filtering may enhance the performance, it significantly increases the computational cost of the filter [31]. In [31] it has been reported that for N operations needed through the use of the LMS technique in BMFLC filters, $3N^2$ operations are needed for Kalman filtering. For example, if we need 160 operations to extract a tremor through the use of LMS in the BMFLC filtering technique, 76800 operations would be needed if we use Kalman filtering [31]. In [30], it has been reported that if the Kalman filter is utilized in the design of the BMFLC technique, having frequency resolution of the model less than $0.5Hz$ can prevent real-time implementation of the filter (when $512Hz$ sampling rate is assumed as the definition of real-time implementation). Note that for the case of haptic interaction, the sampling frequency is suggested to be at least between $1KHz$ and $1.5KHz$. In addition to the above, as can be seen in [30], [16], using the Kalman filter for BMFLC filtering, the linear state-space model of the system will not be time-invariant. This

does not match with requirements of the classical Kalman filters with guaranteed stability and it has been shown that it can result in an unexpected diverging behavior [32], [33], [34], especially since the measurement and the model are uncertain (which is the case for pathological hand tremor). Finally, it should be added that in order to use the Kalman filtering technique in practice, the covariance matrices for the model and observation uncertainties should be properly tuned based on **knowledge** of existing measurement noises and model uncertainties [32], [33]. The possible diverging behavior of the Kalman filter is closely related to the tuning of the covariance matrices [33]. This makes it even more challenging to use the Kalman+BMFLC technique. As a result, in this paper we propose two new modifications (for the LMS+BMFLC) which can significantly enhance the accuracy of the conventional BMFLC filter (as shown later in this paper) without adding further complications for extracting pathological tremors. The LMS algorithm is shown below:

$$\hat{Y}(t) = \hat{\theta}^T(n)\phi(t) \quad (6)$$

where

$$\hat{\theta}^T(n) = \hat{\theta}^T(n-1) + 2\eta\phi(n)E(t)$$
$$\text{and } E(t) = S(t) - \hat{Y}(t). \quad (7)$$

In (7), η is the LMS corrective gain, $E(t)$ is the estimation error, $S(t)$ is the input signal, $\hat{Y}(t)$ is the estimated signal, $\hat{\theta}$ is the estimation of the coefficient vector of the Fourier combiner model. Since the model is truncated, the estimated signal will be an estimation of the high frequency components of the hand motion $M_{p-i}(t)$ [12], [13], [14].

III. PROPOSED ENHANCED-BMFLC TECHNIQUE

In this section, we indicate two facts that can degrade the performance of the BMFLC filter, then we propose solutions which form the new design called E-BMFLC.

A. Challenges with the Conventional Design of BMFLC

There are two problems associated with the conventional formulation of the BMFLC filter in (4)-(7):

1) Inaccurate Error Calculation: In (7), the error is represented as $E(t) = S(t) - \hat{Y}(t)$, where $\hat{Y}(t)$ is the estimated tremor. However, the input signal $S(t)$ is equal to the modulated hand motion $M_p(t)$, the only measurable characteristic of the hand's motion. It is known that the actual measure of hand tremor $M_{p-i}(t)$ is not accessible and estimating it is the main objective of the filter. Consequently, we cannot obtain the actual error between the hand tremor and the estimated tremor. In the conventional design of BMFLC filter, it is assumed that since the model is truncated, the output of this estimation will converge to the content of the tremor frequency window. Although this assumption is not incorrect, it is not accurate either. In the utilized LMS technique (7), the estimation parameters $\hat{\theta}$ concurrently change in the recursive design of the filter to minimize the estimation error $E(t)$. Consequently, although the considered model is truncated, the changing parameters can bring other frequencies out of the window of interest (i.e. $[\omega_a, \omega_b]$) to make the error between the modulated hand

motion $M_p(t)$ and the filter's output $\hat{Y}(t)$ zero. This reduces the accuracy of the filter since the output of the filter should converge to $M_{p-i}(t)$ not $M_p(t)$. As an example, even if at some point, the output of the filter ideally matches with the actual hand tremor $M_{p-i}(t)$, the LMS technique still observes the existing error $E(t)$ since the error is calculated considering the value of M_p not M_{p-i}. Consequently, the filter tries to move the estimation away from that point (which was ideal) and make the error between M_p and $\hat{Y}(t)$ as small as possible. Based on this, we note the following:

Remark 2. We hypothesize that the aforementioned inaccuracy in error estimation will cause considerable sensitivity to the tuning of the corrective gain η. The reason is that for the conventional design of the BMFLC filter, shown in (4)-(7), increasing the corrective gain makes the dynamics of the LMS algorithm faster (more responsive). This results in higher effort of the filter in pushing the estimated signal closer to M_p and away from M_{p-i} by quickly changing the estimation parameters $\hat{\theta}$. On the other hand, it is known that having small values for the corrective gain η in LMS algorithm decreases the convergence rate and estimation accuracy. Consequently, for the design of the BMFLC filter, either increasing or decreasing the gain can result in higher error. This makes it difficult to find an appropriate gain for the BMFLC filter in estimating pathological tremors. This hypothesis (sensitivity to the change in η) is shown in Section V. •

Remark 3. Note that the features of the pathological tremors are considerably variable compared to physiological hand tremor. Consequently, even if we choose a value for the corrective gain η which works in one situation for the hand tremor of a patient, it does not necessarily work for the same patient, in the same session under slightly different condition which can change the characteristics of the hand tremor. The reason is that the new tremor signal may need a different value of η. In other words, considerable variability in the characteristics of pathological tremor necessitate having low sensitivity to the choice of η factor. For the case of physiological tremor, since the variability is not as much as the one for pathological tremor, the inaccuracy might be less. Analyzing the performance of the BMFLC filter for the case of physiological tremor is out of the scope of this paper. The mentioned sensitivity issue is shown in Section V for the case of pathological tremor. •

Remark 4. In addition to the above, since the frequency range of pathological tremor is closer to the voluntary components (in comparison with physiological tremor), higher η values can more easily push the output away from $M_{p-i}(t)$, in the design of the conventional BMFLC filter. •

Remark 5. Since the calculated error for the conventional BMFLC filter $E(t)$ is the difference between the whole modulated hand motion $M_p(t)$ and the estimated tremor $\hat{Y}(t)$, it is not an appropriate measure of accuracy for the model considered in the LMS technique. Consequently, it is not possible to evaluate the performance of the filter and the chosen parameters by monitoring the error $E(t)$. The error might be quite high while the output still matches with the hand tremor.•

Considering the above remarks, there is a need to enrich the model in a way that (a) represents less sensitivity to η, and (b) provides a proper measure of modelling accuracy.

2) Infinite Memory: The other problem of conventional BMFLC filtering is the considered infinite memory of the filter for estimating the coefficients of the truncated Fourier combiner model. Considering (7), the dynamics of the recursive formulation used to estimate the hand tremor keeps the impact of old information similar the one of new information. In other words, the estimated values in the current time sample get affected by all old values *in a recursive manner*. Considering that the regressors model used in the design of BMFLC filter is based on the Fourier linear combiner, having infinite memory means that we have assumed a periodic nature for the tremor. This is the main assumption of conventional BMFLC filters. However, due to the considerable variability in pathological tremor, although assuming a quasi-periodic nature could be correct, the assumption of completely periodic model is not valid. Keeping the impact of old information similar to the new one and trying to find a Fourier combiner model for the whole signal, means that the behavior of the signal is assumed to be periodic and the whole input signal (from the $t = 0$ to the current time sample) can be modelled by one Fourier combiner. Consequently, if the input signal has a specific pattern at the beginning of time, this pattern will be repeated in future estimation of the tremor. This phenomenon is called "Old Tremor Projection (OTP)" in this paper and can considerably reduce the accuracy of the estimation, over time. The existence of OTP is discussed in Section V.

B. Enhanced-BMFLC Filter

In this part, we propose E-BMFLC filter to deal with the aforementioned issues in two phases of enhancement.

Phase #1) Harmonic Model Enrichment:
To deal with incorrect error calculation, we propose to first use an enriched model and then extract the tremor out of the enriched model. This allows us to isolate modelling and tremor extraction steps. The following steps are taken:

Step I: in the first step, instead of using a truncated model considering the frequency window of the tremor $[\omega_a, \omega_b]$, the whole frequency spectrum of the "modulated signal" $M_p(t)$ is modelled using the frequency window of $[\omega_{min}, \omega_{max}]$. ω_{min} is the minimum frequency which is considered in the spectrum of $M_p(t)$, and ω_{max} is the maximum frequency of it. In this paper, ω_{min} is considered to be 0 Hz and ω_{max} is considered to be 20 Hz for the acceleration data of patients' hands. Considering L number of harmonics for the Fourier combiner model of $M_p(t)$, when $L = \beta(\omega_b - \omega_a) + 1$, we have:

$$M_p(t) = \theta_{Mp}^T \phi_{Mp}(t), \tag{8}$$

$$\text{where} \quad \phi_{Mp}(t) =$$
$$\left[\sin(\omega_{min}t + \tfrac{0}{\beta}t), \ \dots \ , \sin(\omega_{min}t + \tfrac{\beta(\omega_{max}-\omega_{min})}{\beta}t), \right.$$
$$\left. \cos(\omega_{min}t + \tfrac{0}{\beta}t), \ \dots \ , \cos(\omega_{min}t + \tfrac{\beta(\omega_{max}-\omega_{min})}{\beta}t) \right]^T, \tag{9}$$

$$\theta_{Mp} =$$
$$\left[\lambda_0, \ ... \ ,\lambda_{\beta(\omega_{max}-\omega_{min})}, \vartheta_0, \ ... \ , \vartheta_{\beta(\omega_{max}-\omega_{min})}\right]^T. \quad (10)$$

The complete model of the input signal (8) is then used in recursive LMS algorithm for the filter, as follows:

$$\hat{M}_p(t) = \hat{\theta}_{Mp}^T(n)\phi_{Mp}(t) \quad (11)$$

where $\quad \hat{\theta}_{Mp}^T(n) = \hat{\theta}_{Mp}^T(n-1) + 2\eta\,\phi_{Mp}(n)E_{Mp}(t)$
$$\text{and } E_{Mp}(t) = M_p(t) - \hat{M}_p(t). \quad (12)$$

In (11),(12), $\hat{M}_p(t)$ is the estimation of $M_p(t)$. Also, E_{Mp} is the difference between the estimated value $\hat{M}_p(t)$ and $M_p(t)$. In addition, $\hat{\theta}_{Mp}^T(n)$ is the coefficient vector for the estimated model for M_p. Consequently, the estimation error E_{Mp} is a real measure of accuracy for the LMS algorithm (in contrast with the conventional BMFLC). Accordingly, we can monitor/utilize E_{Mp} to evaluate the efficacy of the filter. In addition, gradually increasing the corrective gain η results in a more accurate estimation up to a point that the measure of accuracy E_{Mp} shows an acceptable matching between the considered Fourier model for M_p and the real value of M_p. In summary, using the enriched model, the behavior of the filter is more predictable in comparison with the conventional BMFLC and the tuning procedure of η is more straightforward.

Step II): After finding an accurate model for the modulated signal M_p, now we can consider different band-limited windows of frequency to extract various frequency ranges (considering the need of the application). In fact, using the proposed technique, the signal modelling and frequency truncation are decoupled, while in the conventional formulation of BMFLC filter these two steps were fused. In this paper, we considered two frequency ranges: $[\omega_{a-v}, \omega_{b-v}]$ for the voluntary component of the motion and $[\omega_{a-i}, \omega_{b-i}]$ for the involuntary component of the motion. We have:

$$\omega_{max} \geq \omega_{b-i} \geq \omega_{a-i} \geq \omega_{b-v} \geq \omega_{a-v} \geq \omega_{min} \geq 0 \quad (13)$$

Accordingly, the estimation of the voluntary component of the motion (i.e. $\hat{M}_{p-v}$), and the involuntary component of the motion (i.e. $\hat{M}_{p-i}$) can be obtained as given below:

$$\hat{M}_{p-v}(t) = \hat{\theta}_{Mp-v}^T(n)\phi_{Mp-v}(t)$$
$$\hat{M}_{p-i}(t) = \hat{\theta}_{Mp-i}^T(n)\phi_{Mp-i}(t) \quad (14)$$

$$\hat{\theta}_{Mp-v}^T(n) = \left[\hat{\theta}_{Mp}(n)\{i=\gamma_0\},...,\hat{\theta}_{Mp}(n)\{i=\gamma_1\},\right.$$
$$\left.\hat{\theta}_{Mp}(n)\{i=\gamma_2\},...,\hat{\theta}_{Mp}(n)\{i=\gamma_3\}\right], \quad (15)$$

$$\hat{\theta}_{Mp-i}^T(n) = \left[\hat{\theta}_{Mp}(n)\{i=\gamma_4\},...,\hat{\theta}_{Mp}(n)\{i=\gamma_5\},\right.$$
$$\left.\hat{\theta}_{Mp}(n)\{i=\gamma_6\},...,\hat{\theta}_{Mp}(n)\{i=\gamma_7\}\right], \quad (16)$$

$$\phi_{Mp-v}^T(n) = \left[\phi_{Mp}(n)\{i=\gamma_0\},...,\phi_{Mp}(n)\{i=\gamma_1\},\right.$$
$$\left.\phi_{Mp}(n)\{i=\gamma_2\},...,\phi_{Mp}(n)\{i=\gamma_3\}\right], \quad (17)$$

$$\phi_{Mp-i}^T(n) = \left[\phi_{Mp}(n)\{i=\gamma_4\},...,\phi_{Mp}(n)\{i=\gamma_5\},\right.$$
$$\left.\phi_{Mp}(n)\{i=\gamma_6\},...,\phi_{Mp}(n)\{i=\gamma_7\}\right]. \quad (18)$$

In (15)-(18), $\hat{\theta}_{Mp}(n)\{i=k\}$ and $\phi_{Mp}(n)\{i=k\}$ are the k_{th} element of $\hat{\theta}_{Mp}$, and ϕ_{Mp} vectors at n_{th} time stamp, respectively. Also, we have:

$$\gamma_0 = \beta(\omega_{a-v}-\omega_{min})+1, \gamma_1 = \beta(\omega_{b-v}-\omega_{min})+1,$$
$$\gamma_2 = L+\gamma_0, \ \gamma_3 = L+\gamma_1, \gamma_4 = \beta(\omega_{a-i}-\omega_{min})+1,$$
$$\gamma_5 = \beta(\omega_{b-i}-\omega_{min})+1, \gamma_6 = L+\gamma_4, \ \gamma_7 = L+\gamma_5. \quad (19)$$

Consequently, the Fourier-based signal modelling and tremor extracting are decoupled. This allows us to first accurately model the modulated signal M_p, and then extract M_{p-i} and M_{p-v}. Consequently, more precise extraction of tremor and less sensitivity to the choice of η are expected. This is statistically demonstrated in Section V.

Phase #2) Memory Manipulation

Here we propose to use windowed memory instead of the conventional infinite memory for the filter. This allows us to adapt better to change in characteristics of the tremor. The sliding memory window results in greater impact from recent values than from old values. For this purpose the recursive formulation of the filter (12) is modified as

$$\hat{\theta}_{Mp}^T(n) = \rho\hat{\theta}_{Mp}^T(n-1) + 2\eta\,\phi_{Mp}(n)E_{Mp}(t)$$
$$\text{where } E_{Mp}(t) = M_p(t) - \hat{M}_p(t), \quad (20)$$
$$\rho = \sqrt[\delta]{\alpha}, \quad \text{and } \delta = \frac{1}{\Delta T}T_p.$$

In (20), ρ defines the pole of the discrete dynamics of the memory windowing for the filter in the Z-domain. The lower the ρ value, the faster the forgetting dynamics will be. This parameter can directly be chosen based on the desired speed that we would like to forget older data (which correlates with the variable nature of the signal to be filtered). Based on our observation which will be reported later in this paper, for extracting pathological tremor of PD and ET patients, $\rho = 0.999$ can be used as the default value which can significantly enhance the performance of the filter. Using (20), we can tune the ρ value when (a) the sampling frequency is different from the one chosen in this paper; and (b) we would like to filter a signal with a different variable nature compared with pathological hand tremor of PD and ET patients. In (20), ΔT is the sampling time (in seconds), T_p is the width of the considered memory window (in seconds), and α is the considered minimum gain within the time window which corresponds to the latest value in the window. The suggested default value for ρ is calculated as follows. The width of the memory window is considered to be $T_p = 2s$. This means that we want to consider a window of $2s$ for keeping the impact of past
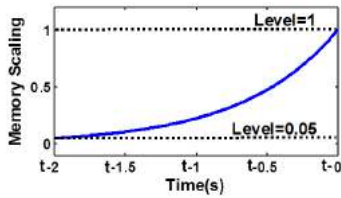
Fig. 3. Sliding memory window. $t-2$ refers to 2 seconds before the current time stamp.

values. Here, **"impact"** corresponds to having scaling gain more than α whose default value is set at 5%. For our clinical experiment, the sampling frequency was 1.5 KHz which means that $\Delta T = (1/1500)s$. The resulting sliding memory window for the designed filter is shown in Fig. 3.

This technique gradually forgets the old information affecting tremor estimation and uses recent data from a limited past time-window. Consequently, the assumption of periodic behavior is relaxed and it is just limited to the considered time-window. As a result, the signal can behave in a "quasi-periodic" manner without violating the assumptions of the designed filter. The combination of the proposed *Harmonic Model Enrichment* and *Memory Manipulation* forms the proposed design for E-BMFLC.

IV. PROPOSED AHR ARCHITECTURE

In this section, the E-BMFLC filter is used in the design of a new therapeutic architecture for pathological tremor patients. The architecture is called Augmented Haptic Rehabilitation (AHR) and performs the following two actions:

- **Action 1)** damping out the extracted hand tremor to avoid amplification of the tremor energy and enhance patient-robot interaction safety;
- **Action 2)** assisting the voluntary component of motion to help the patient in finishing therapeutic tasks.

The modulated force designed by AHR architecture is

$$F_M(t) = F_{R-i}(t) + F_{A-v}(t), \tag{21}$$

where F_M is the modulated force field applied by the rehabilitation robot to the patient's hand; $F_{R-i}(t)$ is the resistive component designed to "damp out" the tremor energy based on the definition of dissipative haptic systems [35]; and $F_{A-v}(t)$ is the assistive component designed to help the patient in finishing the task. The designs of $F_{R-i}(t)$ and $F_{A-v}(t)$ are given in the rest of this section.

A. Modulated Force Field

To damp out the tremor energy, $F_{R-i}(t)$ is calculated as

$$F_{R-i}(t) = B(t)\hat{V}_{p-i}. \tag{22}$$

In (22), $\hat{V}_{p-i}$ is the estimated velocity of the tremor calculated using the proposed E-BMFLC filter. $B(t)$ is the adaptive damping coefficient. This design realizes a viscous environment in the frequency range of the tremor. Consequently, F_{R-i} acts like a damper for the hand tremor and dissipates the corresponding energy. The adaptation

rule to calculate $B(t)$ for each patient is based on a performance measure corresponding to the severity of the tremor (explained later in this section). In addition, to assist the patient's motion in the frequency range of voluntary movement (extracted by E-BMFLC) $F_{A-v}(t)$ is applied to help the patient in following a desired therapeutic trajectory, as

$$F_{A-v}(t) = C(t)E_{p-v}, \\ \text{where,} \quad E_{p-v} = X_{des} - \hat{X}_{p-v} \tag{23}$$

In (23), $\hat{E}_{p-v}$ is the trajectory tracking error, $C(t)$ is the adaptive coordinative gain, X_{des} is the desired position trajectory which should be tracked by the patient, and $\hat{X}_{p-v}$ is the estimated position of the voluntary component (calculated by E-BMFLC). The adaptation rule to calculate $C(t)$ for each patient is based on a performance measure that corresponds to the accuracy of trajectory tracking which is explained later in this section.

B. Performance Measures

In order to calculate $B(t)$ and $C(t)$ for each patient, two performance measures PM_i and PM_v are defined for the proposed resistive and assistive components of the modulated force field, respectively. PM_i provides a quantitative measure of the severity of hand tremor during a rehabilitation task, and PM_v provides a quantitative measure of accuracy for tracking the rehabilitation trajectory using the voluntary component of the hand motion.

The design of PM_i is as follows:

$$PM_i(t) = \frac{\xi_{tremor}(t)}{\xi_{max-1}}. \tag{24}$$

In (24), ξ_{tremor} is the real-time measure of the energy of the involuntary hand velocity. To eliminate time-dependence of $PM_i(t)$, windowed energy is considered for ξ_{tremor}:

$$\xi_{tremor}(t) = \int_{t-T_w}^{t} \hat{V}_{p-i}(\tau)^2 \, d\tau. \tag{25}$$

In (25), T_w is the width of the time window which is considered to be 10 s in this paper. In addition, ξ_{max-1} is a rough estimate of the maximum value for ξ_{tremor}, designed to normalize the proposed performance measure. ξ_{max-1} can be achieved through a preoperative test when the patient is asked to hold/move the robotic handle while the force field is turned off. The ultimate goal is to increase the damping coefficient $B(t)$ until ξ_{tremor} converges to a small value. The design of PM_v is as follows:

$$PM_v(t) = \frac{\xi_{E-track}(t)}{\xi_{max-2}}. \tag{26}$$

In (26), $\xi_{E-track}$ is the energy of the tracking error of the voluntary component while considering an acceptable tracking error (i.e. E_{min}). To eliminate time-dependence of $PM_v(t)$, windowed energy is considered for $\xi_{E-track}$:

$$\xi_{E-track}(t) = \int_{t-T_w}^{t} (E_{p-v}(\tau) - E_{min})^2 \, d\tau. \tag{27}$$

In (27), E_{min} is an acceptable threshold for the tracking error which is considered to be 10 percent of the maximum

amplitude of the desired trajectory. Also, E_{p-v} is the tracking error of the voluntary component of the patient's hand motion. In addition, in (26), ξ_{max-2} is the normalizing maximum value for the tracking error which is calculated prior to the operation. The value is achieved assuming that the patient is completely incapable of tracking the target (worst case scenario). The ultimate goal is to gradually increase $C(t)$ using the second adaptation rule (explained later) until $\xi_{E-track}$ converges to a small value.

C. Adaptation Rules

Two adaptation rules are proposed to tune $B(t)$ and $C(t)$ based on the needs of the patient:

The First Adaptation Rule: The goal of the first rule is to gradually increase the dissipation gain $B(t)$ for the tremor and keep PM_i under control to make it as small as possible that results in avoiding TA. The adaptation rule is:

$$B(t) = \mu_i(t)B_{max}, \tag{28}$$

$$\text{where} \quad \mu_i(n) = g_i\mu_i(n-1) + PM_i\Delta_i. \tag{29}$$

In (28), B_{max} is the maximum damping factor considered for dissipating the hand tremor. This value can be tuned based on the capabilities of the utilized robot. In this paper, the default value for B_{max} is $250N.s/m$. In addition, μ_i is the adaptive scaling gain which is calculated using (29) based on the severity of the tremor. In (29), g_i is the forgetting factor and Δ_i is the growth rate constant for $B(t)$. To better understand the functionality of the proposed rule, first assume $g_i = 1$. In this case, if the patient shows a severe tremor (which means $PM_i \rightarrow 1$) the adaptive scaling gain μ_i gradually increases with the rate of Δ_i. Increasing μ_i results in having higher $B(t)$ which results in having less tremor and better performance measure PM_i. This reduces the growth rate of $B(t)$. At the same time, considering the forgetting factor g_i slightly less than unity results in slowly forgetting early information and allowing the patient to experience a lower dissipation, if he/she represents a less severe tremor after some point. Finally, μ_i will converge to an equilibrium value which is specifically achieved for this patient to minimize his/her tremor. To better understand the functionality of g_i, suppose that the hand tremor suddenly stops at some point. This does not of course happen in practice. We are assuming it to clarify the behavior of g_i. In this case, if $g_i = 1$, the dissipative gain $B(t)$ will stay at the previous value, while there is no tremor. However, by having g_i slightly less than unity the dissipative gain $B(t)$ will gradually reduce. Note that if at any point, the severity of the tremor changes, this will be observed by PM_i and it results in changing μ_i and setting a new equilibrium point for it. Consequently, taking advantage of having both g_i and Δ_i, an appropriate value for $B(t)$ can be achieved which minimizes PM_i while providing minimum needed resistance. This technique is called Energy-based Resist-as-Needed (ERN) approach. The default value for g_i is 0.99995. This value can make μ_i less than half in 15 s when $PM_i = 0$, considering sampling time of 1 KHz. Also, the default value for Δ_i is 0.0005 which can result in reaching the maximum $B(t)$ in 2 s when $g_i = 1$ and $PM_i = 1$.

The Second Adaptation Rule: The goal of the second rule is to gradually increase the assistive coordination gain $C(t)$ for the voluntary component and keep PM_v as small as possible. This will result in having an acceptable tracking performance in an assist-as-needed manner. The ultimate purpose is to provide the patient with minimum assistance just needed to perform the task and not to provide him/her with too much assistance. If too much assistance was provided, the patient would rely on the robot and would not get involved in the interactive procedure. The rule is achieved using similar concept mentioned above as

$$C(t) = \mu_v(t)C_{max}, \tag{30}$$

$$\text{where} \quad \mu_v(n) = g_v\mu_v(n-1) + PM_v\Delta_v. \tag{31}$$

In (30), C_{max} is the maximum coordination factor considered for delivering assistance to the voluntary component. This value can be tuned based on the capabilities of the utilized robot. The default value for B_{max} is 800 N/m. In addition, $\mu_v(t)$ is the adaptive scaling gain which is calculated using (31) based on the severity of the coordination deficit. In (31), g_v is the forgetting factor and Δ_v is the growth rate constant for $C(t)$. The functionality of the adaptation rule given in (31) is similar to that of (29). The goal is to find the minimum assistance needed for the patient. Having g_v slightly less than unity allows us to always challenge the patient and try to keep him/her involved in the loop. In fact, this choice of g_v allows for evaluating the patient's capability in tracking the trajectory and automatically tuning $C(t)$ to provide corresponding assistance. If we consider $g_v = 1$ and the patient's trajectory tracking is inaccurate at the beginning of the task, μ_v will converge to a high equilibrium value and will stay there. In this situation, if trajectory tracking becomes more accurate, since we had $g_v = 1$, the assistive gain $C(t)$ will not be reduced and the robot will keep on providing assistance. However, by considering g_v slightly less than unity the coordination gain will gradually drop when the patient starts to behave in a more accurate manner. This results in an assist-as-needed approach which we call Energy-based Assist-as-Needed (EAN) technique. The default values for g_v and Δ_v are 0.9998 and 0.0002, respectively. The designed AHR system is shown in Fig. 2.

V. FILTER EVALUATION AND CLINICAL STUDY

In this section, the clinical evaluation of E-BMFLC filter is presented. The goal is to evaluate the accuracy, and the corresponding sensitivity to the tuning of η and intra-patient variability, in comparison with BMFLC filter.

A. Demographic data

This study includes 27 patients (14 PD, and 13 ET). The patients were aged from 36 to 86 (mean: 67.85, S.D.=11.46). The population involved 17 males and 10 females. Patients were recruited from the Movement Disorders Centre at University Hospital, London Health Sciences
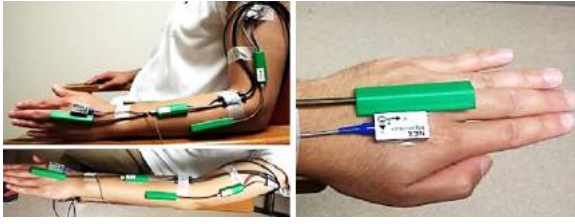
Fig. 4.   Multi-sensor experimental setup for tremor data collection.

Centre (London, Ontario, Canada). The study protocol was approved by the Research Ethics Board at Western University. Written consent forms and details of the protocol were provided to the patients prior to their participation.

B. Experimental Setup and Task

The experimental setup (shown in Fig. 4) consists of a full upper-limb kinematic measurement system from *Biometrics Ltd*. Motion sensor data was collected at 1500Hz and transmitted to the PC interface *MyoResearch* from *Noraxon*. In this paper, we used measurement data of a 3 DOF Cartesian accelerometer on hand. Each patient has been asked to perform a random target tracking task in free space for 20 seconds by repetitively moving the hand from nose to a pen showing the target. The target positions are set such that the patient needs to fully stretch out his/her arm. After one 20-second episode of target tracking the patient is asked to perform other tasks in series (each for 20 seconds) i.e. holding an empty cup, holding a loaded cup, resting hands on lap, resting hands on a support table. These tasks are chosen to change their tremor conditions and trigger different characteristics. This allows us to evaluate their tremor in different situations. The procedure is repeated three times (three trials) for each patient. Consequently, for all 27 patients we have 3DOF acceleration for 3 separated episodes. As a result, each patient provides 9 sample signals of 20-second target tracking. Considering all 27 patients, we have 234 sample data, in total.

C. Evaluation Protocol

An evaluation protocol is needed to be repeated for all sample data. The question to be addressed is: "what are the ideal references (for voluntary and involuntary motions) which should be considered to calculate the accuracy and sensitivity?". For this goal, the following protocol has been conducted. For each sample signal:

Step 1) Fast Fourier Transform (FFT) is calculated.
Step 2) A 7th-order linear polynomial is fitted to the absolute value of the calculated FFT.
Step 3) The analytical derivative of the 7-order polynomial is calculated. This is used to find the two suprema of the polynomial which correspond to the peaks in the central frequencies of the voluntary and the involuntary components. Also, the cut-off frequency that can separate the components is calculated.
Step 4) The internal product of the FFT of the signal and a separating vector V_{sep} with the same size is calculated. V_{sep} has values equal to one for frequency

less than the cut-off frequency and zero for frequencies higher than that. The result is the ideal FFT of the voluntary component of motion.
Step 5) The same procedure is repeated while replacing the separating vector by $1 - V_{sep}$. The result is the FFT of the involuntary component of the hand motion.
Step 6) The achieved ideal FFT vectors of the voluntary and involuntary motions are named $H_v(f)$ and $H_i(f)$, respectively. f is frequency in Hz.
Step 7) The inverse FFTs of both the voluntary and involuntary components are calculated. These are used as the ideal references for evaluating the output of the filters. The achieved ideal references in the time-domain are named $R_v(t)$ for the voluntary component and $R_i(t)$ for the involuntary component. Note that the mentioned procedure is a post-processing technique representing how to realize an offline ideal filter.

The mentioned procedure is displayed in Fig. 5, for motion in the X-direction of participant #21.

D. Method and Evaluation Metrics

In this part, the method used to evaluate and compare the performance of the filters is discussed. After calculating the cut-off frequencies and finding the references to perform evaluation in frequency-domain and in time-domain, both the BMFLC and E-BMFLC filters have been implemented in real-time for three corrective gains η, as explained as follows. Based on our observations, $\eta = 0.004$ is a rational value to be considered for the filters. This observation is made by checking 10 random signals out of the 234 items of data. To evaluate the sensitivity of the filters to the change in η, and to evaluate/compare the performance of the filters, we run both BMFLC and E-BMFLC techniques for two more η values, which are 0.004 $\pm 50\%$. It should be noted that changing the η value *considerably more* than 50% of the nominal value (i.e. 0.004) resulted in diverging behavior for the conventional BMFLC filter in some of the mentioned 10 randomly chosen signals. Although the diverging behavior could be a good validation of the high sensitivity of the conventional filter, it would not allow us to quantitatively compare the sensitivity of the two filters. As a result, 50% deviation is considered to analyze and compare the sensitivity of the two filters (BMFLC and E-BMFLC) to the change in η value.

As a result of the above mentioned method, each signal (out of the 234 signals) is filtered for 3 times by the BMFLC filter and for other 3 times by the E-BMFLC filter.

The Normalized RMSE (NRMSE) values of the extracted tremors (applying both the BMFLC and E-BMFLC filters) are calculated in the time-domain, using the ideal reference $R_i(t)$. Also, the NRMSE values of the extracted tremors (applying both the BMFLC and E-BMFLC filters) are calculated in the frequency-domain using $H_i(t)$.

Consequently, applying the BMFLC filter on each hand signal, we calculate three NRMSE values in the time domain which corresponds to the three η values; also, we have three NRMSE values in the frequency domain. In
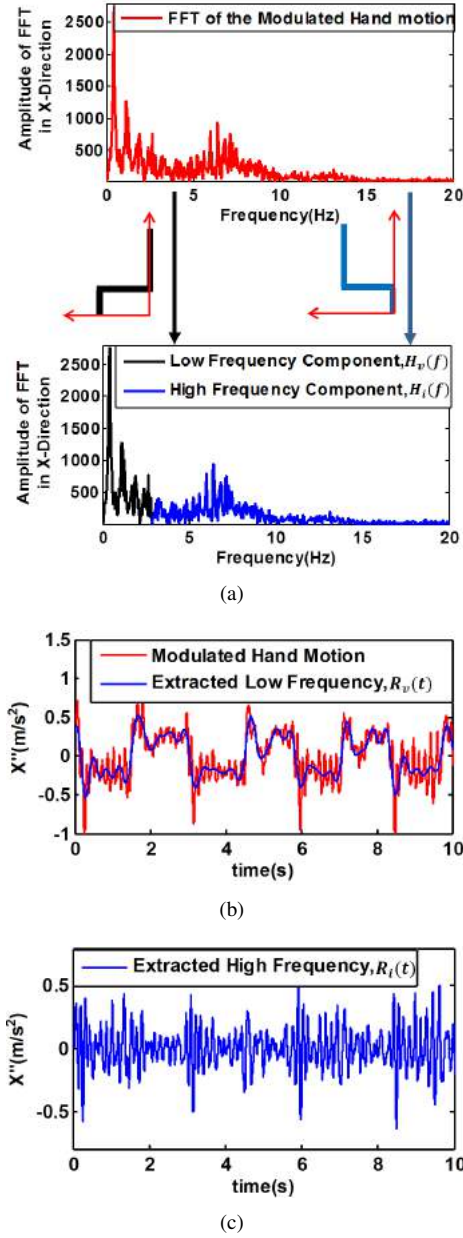
Fig. 5. The results of the proposed post-processing protocol to calculate $R_v(t)$, $R_i(t)$, $H_v(f)$, $H_i(f)$ for participant #21 in the X-direction. (a) The visualization of the proposed protocol; (b) the modulated hand acceleration versus the extracted voluntary component $R_v(t)$; (c) the extracted involuntary component of motion $R_i(t)$.

addition, applying the E-BMFLC filter on each signal we will calculate three NRMSE values in the time-domain and three NRMSE values in the frequency-domain. Using the achieved NRMSE values, six metrics are designed which will be used in the next part ("Part E") to statistically compare the performance of the filters.

Metrics #1 *and* #2) In order to calculate the extent of improvement potentially achieved using the proposed E-BMFLC filter, the first metric is calculated for all 234 signals in the time-domain, as follows:

$$IMP_{Error(t)} = \frac{NRMSE_{conv-t} - NRMSE_{enhanced-t}}{NRMSE_{conv-t}}, \quad (32)$$

In (32), $NRMSE_{conv-t}$ corresponds to the conventional BM-

FLC filter. It is the minimum NRMSE value (best performance) in the time-domain, considering the three NRMSE values calculated by applying the three η values. Consequently, for each signal (out of the 234 signals) we have one $NRMSE_{conv-t}$ value. In addition, $NRMSE_{enhanced-t}$ corresponds to the proposed E-BMFLC filter. It is the minimum NRMSE value achieved in the time-domain out of the three NRMSE values calculated by applying the three η values. As a result, $IMP_{Error(t)}$ represents the improvement achieved for tracking error in the time-domain, by applying the E-BMFLC filter and in comparison with the BMFLC filter. Consequently, we have 234 $IMP_{Error(t)}$ values and the statistical distribution of it will be analyzed in Part E of this subsection. $IMP_{Error(t)} = 0$ indicates no improvement, and $IMP_{Error(t)} = 1$ indicates 100% improvement.

The same procedure is repeated to calculate the second metric which is the potential improvement achieved by applying the E-BMFLC filter, in the frequency-domain. The definition of the second metric is:

$$IMP_{Error(f)} = \frac{NRMSE_{conv-f} - NRMSE_{enhanced-f}}{NRMSE_{conv-f}}. \quad (33)$$

In (33), $IMP_{Error(f)}$ is the improvement achieved for estimating error in the frequency-domain.

Metrics #3 *and* #4) In addition to the above, to quantitatively evaluate the consistency of the filter in estimating hand tremor and statistically compare the filters from the point of view of the sensitivity to the choice of η, the third and forth metrics are designed. The third metric is:

$$IMP_{\eta VAR(t)} = \frac{V_{conv-t} - V_{enhanced-t}}{V_{conv-t}}. \quad (34)$$

In (34), V_{conv-t} is the variance of the three NRMSE values for each signal which correspond to the considered three values of η for the conventional BMFLC filter, in the time domain. Also, $V_{enhanced-t}$ is the variance of the three NRMSE values which correspond to the considered three values of η for the proposed E-BMFLC filter, in the time domain. Consequently, $IMP_{\eta VAR(t)}$ is a quantitative metric which can tell us how much improvement is achieved applying E-BMFLC filter (in comparison with conventional BMFLC filter), from the point of view of sensitivity to the change in η value. Having $IMP_{\eta VAR(t)}$ close to unity means that under the same condition, the E-BMFLC filter demonstrates little performance change (less sensitivity) in comparison to the BMFLC filter. On the other hand, having $IMP_{\eta VAR(t)}$ close to zero means that the E-BMFLC filter behaves similar to the conventional BMFLC filter from the point of view of sensitivity to the change in η. The third metric will be calculated for all 234 signals and the statistical distribution of it will be evaluated in Part E.

The sensitivity of the filters can be also compared in the frequency-domain using the fourth metric, $IMP_{\eta VAR(f)}$, as:

$$IMP_{\eta VAR(f)} = \frac{V_{conv-f} - V_{enhanced-f}}{V_{conv-f}}. \quad (35)$$

In (35), V_{conv-f} is the variance of the three NRMSE values for each signal which correspond to the considered three

values of η for the conventional BMFLC filter, in the frequency-domain. Also, $V_{enhanced-f}$ is the variance of the three NRMSE values which correspond to the considered values of η for E-BMFLC filter, in the frequency-domain.

Metrics #5 *and* #6) We are also interested in comparing the sensitivity of the filters to changes in motion characteristics of patients and account for intra-patient variabilities. For this goal and to evaluate the consistency of the filters in extracting hand tremors of different patients with various characteristics, the fifth and sixth metrics are designed. These metrics show how much improvement is achieved in reducing the variation in performance under different motion conditions associated with different patients. These metrics are achieved for all 27 patients. The fifth metric is:

$$IMP_{\Omega VAR(t)} = \frac{W_{conv-t} - W_{enhanced-t}}{W_{conv-t}}. \qquad (36)$$

In (36), W_{conv-t} is the variance of the nine NRMSE values which correspond to the nine best performances achieved by applying the BMFLC filter for estimating nine motion data for each patient in the time domain. The explanation of how to calculate W_{conv-t} is as follows: For each patient we have 9 measured signals (3DOF measurements for 3 trials). Each signal is filtered using three different values of η. The best performance for filtering each signal is the minimum NRMSE value out of the three NRMSE values achieved by applying the defined three η values. Accordingly, for each signal we have one best performance. Considering nine signals for each patient, we have nine best performances for each patient. The variance of these nine best performances is W_{conv-t} for the BMFLC filter in the time-domain. Consequently, for each patient we have one W_{conv-t} value in the time-domain.

Also, $W_{enhanced-t}$ is the variance of the nine minimum NRMSE values which correspond to the best performances achieved applying the E-BMFLC filter for estimating the nine motion data for each patient in the time-domain. Consequently, for each patient we have one $W_{enhanced-t}$ value in the time-domain. Accordingly, $IMP_{\Omega VAR(t)}$ can be calculated for each patient as given in (36), which is the improvement achieved in reducing the variation in the performance by applying the E-BMFLC filter. Finding $IMP_{\Omega VAR(t)}$ for all 27 patients, we can statistically analyze the corresponding distribution. This is done in Part E.

Similarly, the consistency of the filters can be compared in the frequency-domain using the sixth metric, $IMP_{\Omega VAR(t)}$:

$$IMP_{\Omega VAR(f)} = \frac{W_{conv-f} - W_{enhanced-f}}{W_{conv-f}}. \qquad (37)$$

In (37), W_{conv-f} and $W_{enhanced-f}$ are the variance of the nine minimum NRMSE values in the frequency-domain for the BMFLC filter and the E-BMFLC filter, respectively.

E. Implementation Results and Statistical Analysis

In this part, first, various aspects of the proposed E-BMFLC filter are separately analyzed. Then, the results of the statistical comparative study on the efficacy of the filter for extracting tremors of 27 patients are given.

I) Analyzing Old Tremor Projections: As mentioned before, one of the challenges with conventional BMFLC filter is the infinite memory of it, besides the assumption of fully-periodic input signal. This can result in repetitive OTPs which can degrade the efficacy. To show the existence of OTPs in the conventional BMFLC filter, and to *isolate* it from other potential sources of error, the following steps are taken. First, motion data for one patient have been randomly chosen. In this case, we chose the hand motion of Participant #4 (a 55 years old male with PD) in the X-direction, during the first trial. While applying no change to the first 3 seconds of the signal, we cut the remaining part of the signal (from $t = 3\ s$ to $t = 20\ s$) and make it zero. This is just to highlight and extract the effect of OTPs. The result of applying conventional BMFLC filter is shown in Fig. 6(a). As can be seen, although the original signal is flattened after $t = 3s$, repetitive projections exist in the estimated value. These are the predicted OTPs. As mentioned, the OTPs are the result of assuming the fully periodic model in BMFLC besides having infinite memory. Applying the proposed memory windowing technique for the same filter ($\rho = 0.999$) results in Fig. 6(b). As can be seen in Fig. 6(b), the OTPs are completely eliminated. This result validates existence of OTPs and effectiveness of the proposed memory windowing technique. In Fig. 6(c), the estimated coefficients of the utilized Fourier combiner are plotted, over time. As it is shown in Fig. 6(c), for the conventional BMFLC filter, the coefficient values still vary after $t = 3\ s$. The reason is that the filter assumes that the complete hand signal from $t = 0$ to the current time stamp should be modelled by a periodic nature. Better view of the coefficients are given in Fig. 7(a). After applying the proposed memory windowing, the coefficients gradually converge to small values (after $t = 3\ s$) eliminating the OTPs. This is shown in Fig. 6(d) and Fig. 7(b).

II) Analyzing Sensitivity to the Design of η: As mentioned earlier, we hypothesize that the design of the proposed E-BMFLC filter is more robust to the change in η value in comparison with BMFLC filter. This is statistically evaluated at the end of this section. Here, an example for one signal is given to discuss the behavior of E-BMFLC and the conventional BMFLC for three different η values (i.e. 0.002, 0.004, 0.006). The data of Participant #4 is analyzed here. For this purpose, we have considered hand motion in the X,Y, and Z directions, for the defined three trials. So, in total we have the following 9 data samples:

- Sample #1: X-direction, Trial #1
- Sample #2: X-direction, Trial #2
- Sample #3: X-direction, Trial #3
- Sample #4: Y-direction, Trial #1
- Sample #5: Y-direction, Trial #2
- Sample #6: Y-direction, Trial #3
- Sample #7: Z-direction, Trial #1
- Sample #8: Z-direction, Trial #2
- Sample #9: Z-direction, Trial #3

The above 9 signals have been used to evaluate both the BMFLC and E-BMFLC filters, while considering the
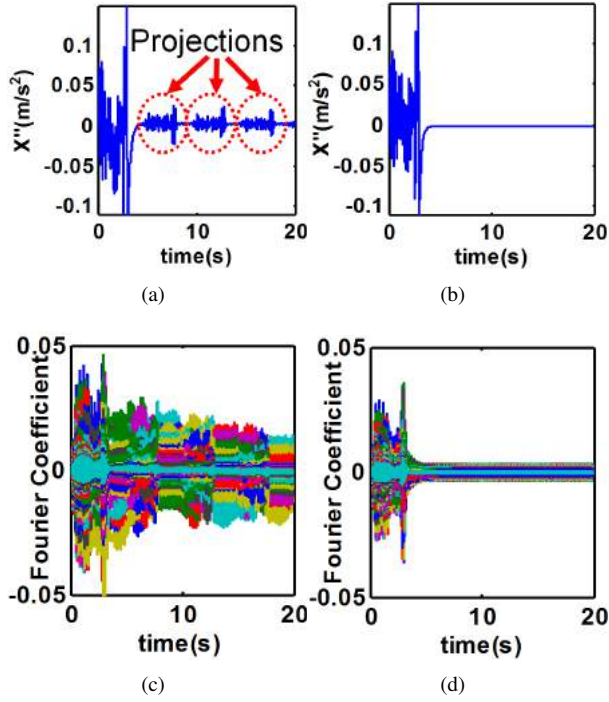
(a)

(b)

(c)

(d)

Fig. 6. (a) The existence of OTPs in the output of BMFLC filter; (b) elimination of OTPs by applying the proposed memory windowing; (c) the estimated coefficients of the Fourier model for the case of BMFLC filtering; (d) the estimated coefficients after applying memory windowing.
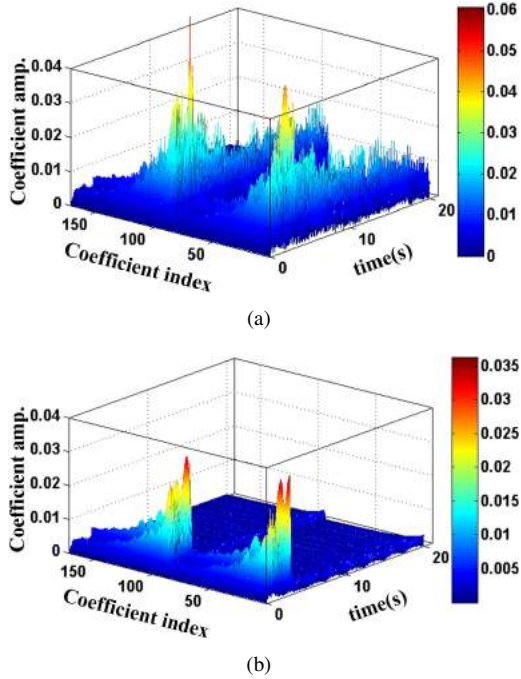

(a)

(b)

Fig. 7. (a) The 3D view of the estimated Fourier coefficients (a) for BMFLC filtering, (b) after applying memory windowing.

defined three η values for each filter and each signal. The corresponding NRMSE values in the time-domain and in the frequency-domain are calculated. The results are shown in Fig. 8. In this figure, red lines correspond to BMFLC filter. Each line is the result of one η value. Also, the blue lines correspond to the proposed E-BMFLC filter.
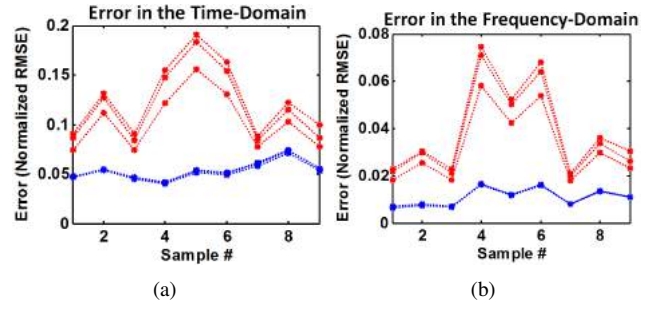

(a)

(b)

Fig. 8. The NRMSE values for the proposed E-BMFLC filter (blue lines) and the conventional BMFLC technique (red lines). Each line corresponds to applying one η value out of the considered three values. (a) Results in the time-domain; (b) results in the frequency-domain.
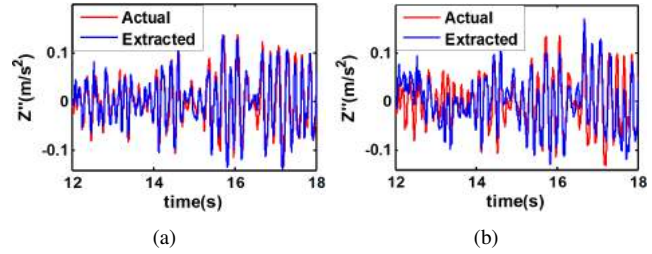

(a)

(b)

Fig. 9. Tremor extraction for Participant #4 in the Z-direction, during the first trial. The red line is the actual hand tremor, and the blue line is the output of the filter. (a) The result of applying the proposed E-BMFLC filter; (b) the result of applying the conventional BMFLC filter.

Considering the results in Fig. 8, the E-BMFLC filter not only provides a *more accurate tremor estimation* (lower average NRSME value), it has represented (a) less performance change (less sensitivity) applying different η values, and (b) less variation in performance applying different inputs (considering different signals). In fact, the difference between the results of using different η values is not even easily distinguishable in the figure for the E-BMFLC filter. However, the performance of the conventional BMFLC filter changes dramatically by changing the η values and by using the same filter for a different data point.

Consequently, it can be concluded that for the considered participant, the E-BMFLC filter has shown a more robust, more accurate and less sensitive performance.

The outputs of the filters are plotted over time for the Z-direction during the first trial, in Fig. 9. As expected, the figure shows more accurate estimation achieved by using the E-BMFLC filter in tracking the hand tremor of this participant when comparing with the conventional BMFLC filter, under the same condition.

To ensure that the achieved conclusion is statistically significant and consistent, we need to evaluate the filters for a group of patients and run a standard statistical test, as given in the following part.

III) Patient-based Evaluation and Statitsical Analysis: In this part, the effectiveness of the proposed E-BMFLC filter is statistically evaluated in comparison with the performance of the conventional BMFLC technique. For this purpose, the statistical distributions of the aforementioned six metrics are evaluated. The average values and standard deviations for the six metrics are calculated. The standard

TABLE I
SUMMARY OF THE STATISTICAL ANALYSIS

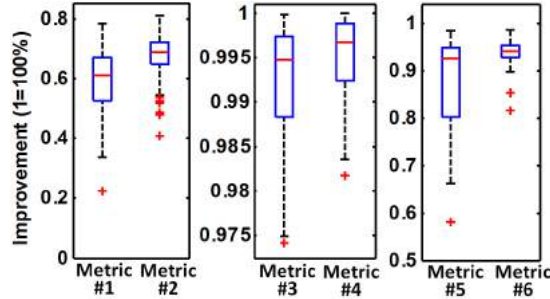|		Average Improvement	Standard Deviation	P-Value
Metric #1	$IMP_{Error(t)}$	59.73%	9.59%	≤ 0.001
Metric #2	$IMP_{Error(f)}$	68.22%	6.03%	≤ 0.001
Metric #3	$IMP_{\eta VAR(t)}$	98.68%	4.36%	≤ 0.001
Metric #4	$IMP_{\eta VAR(f)}$	99.11%	3.29%	≤ 0.001
Metric #5	$IMP_{\Omega VAR(t)}$	86.41%	14.27%	≤ 0.001
Metric #6	$IMP_{\Omega VAR(f)}$	93.20%	3.52%	≤ 0.001

Fig. 10. Statistical distribution of the six improvement metrics.

statistical *T-test* is utilized to analyze the significance of the calculated improvements. The results are summarized in Table I. In addition, the corresponding box plots of the distributions are plotted in Fig. 10 for metrics #1 to #6. As can be seen in Table I, the average improvement achieved for NRMSE in the time-domain ($IMP_{Error(t)}$) is 59.73% and the standard deviation is 9.59%. Also, the average improvement for NRMSE value in the frequency-domain ($IMP_{Error(f)}$) is 68.22% with standard deviation of 6.03%. The significance of the results are validated using the *T-test* which results in a p-value < 0.001. This shows that the achieved improvements are statistically significant. The same analysis is performed for other defined metrics and the results are shown in Table I.

Considering the results summarized in Table I, the proposed E-BMFLC filter, has statistically significant improvement in accuracy of the filter for estimating hand tremor. This is interpreted based on the statistical analysis of $IMP_{Error(t)}$ and $IMP_{Error(f)}$. Also, the sensitivity to the change in η, is significantly reduced. This is interpreted based on the statistical analysis of $IMP_{\eta VAR(t)}$ and $IMP_{\eta VAR(f)}$. In addition, the proposed filter shows considerable improvement in reducing the sensitivity to the change in tremor characteristics of different patients. This is interpreted based on the statistical analysis of $IMP_{\Omega VAR(t)}$ and $IMP_{\Omega VAR(f)}$. All the results are statistically significant in both the time-domain and the frequency-domain. Consequently, the proposed filter consistently shows significant improvement in extracting hand tremors of patients living with PD and ET. This validates the hypotheses of this paper.

VI. EXPERIMENTAL EVALUATION OF THE AUGMENTED HAPTIC REHABILITATION ARCHITECTURE

In this section, the proposed AHR system is implemented and experimentally evaluated. Upper-limb rehabilitation robot from Quanser Inc. is used, shown in Fig. 2. The user wears a head-mounted display visor which provides visual cues and the location of the moving target to track. The experiment is designed to evaluate different features of the AHR system including the proposed adaptive assistance and resistive algorithms. It should be noted that in pathological tremor patients, the involuntary movement is due to involuntary activation of hand muscles which results in an involuntary force field. Consequently, in this experiment, while a healthy user handles the robot, the tremor of participant #21 is chosen randomly to design a tremor-like force field for the user to mimic the interaction between a tremor patient and the system. It should be highlighted that the generated force field in this experiment might be different from the one felt by the user during data collection. As mentioned, in this section we aimed to analyze the performance of the proposed AHR system. As a result it was needed to make a tremor-like force field to analyze the reactions of the system. For this purpose, the data collected for Participant #21 has been used as a model to make the force field which represents a realistic frequency content of a human with pathological hand tremor.

A. Experiment Design

The experiment is designed in three phases. In the **first phase** ($0s \leq t < 27s$), the user holds the robot while the robot perturbs the user's hand by applying the designed tremor-like force field. During this phase, the robotic therapy is turned off and no assistive/resistive force is delivered to the user. It is expected that the user's hand continues shaking in a tremor-like manner. During the **second phase** ($27s \leq t < 60s$), the designed resistive force field is turned on. It is expected that the intensity of the dissipative force gradually increases due to the proposed adaptation rule (28) and (29). This should result in a reduction in the amplitude of the hand tremor. During the **third phase** ($t \geq 60s$), the assistive force field is also turned on. It is expected that during this phase, the intensity of the assistive force field gradually increases (due to the proposed corresponding adaptation rule (30) and (31)). This should result in an increase in the amplitude of the low-frequency of the hand motion and a reduction in the tracking error.

It should be highlighted that during the third phase, for $t \leq 100s$, the user just holds the robotic handle and does not try to track the target trajectory in order to mimic the behavior of a severely impaired patient. Consequently, the robot should take the full authority, increase the coordinative gain and push the user's hand towards the correct path of motion. After $t = 100s$, the user starts to act like a less-impaired patient by putting effort in tracking the target. Consequently, if the designed adaptation rule works, it is expected that the intensity of the assistance force field should reduce and the system should give some authority

to the user. This means that the equilibrium point for the coordinative gain should drop after $t = 100s$.

B. Results

The results of the experiment are shown in Figs. 11 and 12. In Fig. 11(a), the hand velocity is shown for the proposed three phases of the experiment. As can be seen in the figure, during the first phase, the hand of the user shakes due to the applied tremor-like force field, while the therapeutic forces are turned off. When the resistive therapy is started (as Phase 2), the amplitude of the hand tremor considerably reduces as expected. The amplitude of the tremor during the second phase is 8.6 times smaller than that during the first phase. This is due to the gradual increase in the dissipative gain which can be seen in Fig. 12(b). In addition to the above, by the start of the third phase in Fig. 11(a), the amplitude of the low-frequency motion increases which is due to the increase in the coordinative gain. The coordinative gain is shown in Fig. 12(a). This results in gradual reduction in the tracking error (as can be seen in 11(b)). The target movement is shown by the solid red line in Fig. 11(b), where the voluntary component of the hand motion is shown by the solid blue line. The total modulated force provided by the proposed controller during the second and the third phases is shown in Fig. 11(c). During the second phase, the aforementioned modulated force has high-frequency components to resist the hand tremor. During the third phase and before $t = 100s$ the modulated force has significant low-frequency components (to guide the user's hand towards the correct path) together with the high-frequency components to resist the hand tremor. Considering Fig. 12(a), after $t = 100s$, when the user starts to act like a less-impaired patient by putting effort in tracking the target, the coordinative gain is significantly reduced (by 64%). This means that the controller detects that the user is more capable of moving the robot (after $t = 100s$) so the adaptive algorithm provides 64% of the authority to the user. Consequently, as can be seen in Fig. 11(c), after $t = 100s$, the low-frequency component of the modulated control force is reduced (which is due to the reduction in the coordinative gain), while still the high-frequency components exists to dissipate the tremor energy. These results match with the expectations and validate the functionality of the architecture.

VII. CONCLUSION

In this paper, a new design of the BMFLC filter was proposed which we have called E-BMFLC technique. The new filter uses an enriched Fourier combiner model together with a windowed memory. The goals were to reduce the error in extracting pathological hand tremor as well as the sensitivity of the filter to the choice of the corrective gain used in the filter and intra-patient variabilities. To evaluate the performance of the filter, recorded hand motions of 27 patients (PD and ET) were used in the comparative study. The proposed E-BMFLC filter showed a statistically-significant improvement (p-value < 0.001) in estimation accuracy, in comparison with the conventional design of
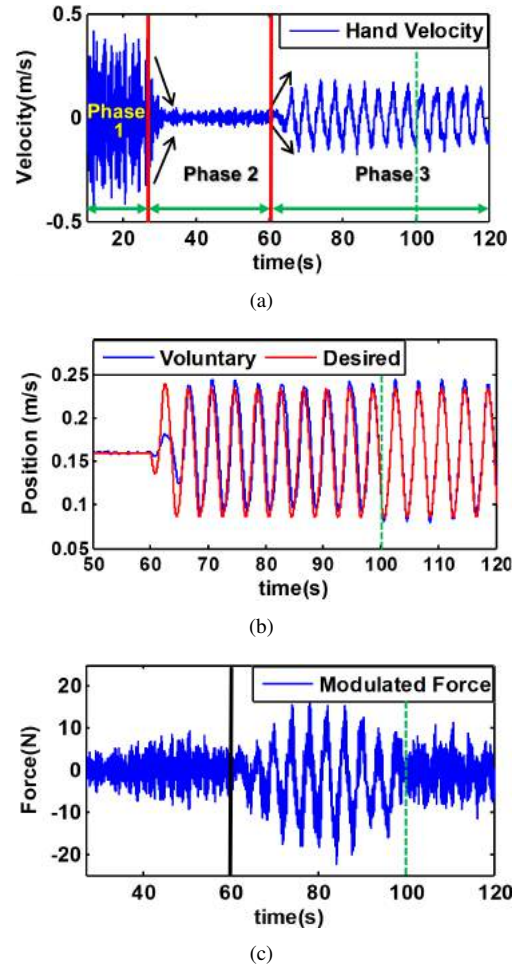

(a)

(b)

(c)

Fig. 11.   Experimental results for the three phases. (a) hand velocity, (b) target tracking, (c) the designed modulated force field.
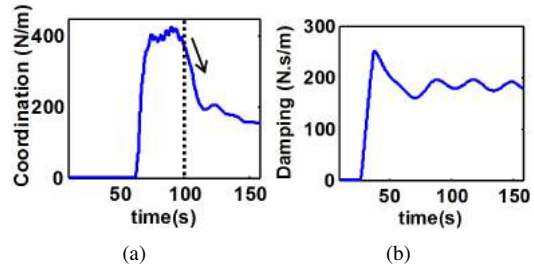

(a)   (b)

Fig. 12.   The designed parameters for the therapy: (a) coordinative gain, (b) dissipative resistive gain.

the BMFLC filter. The tremor tracking accuracy and the sensitivity to the choice of corrective gain and intra-patient variabilities were significantly improved using the proposed filter. In the second part of this paper, the designed filter was utilized in developing a new haptics-enabled rehabilitation strategy, called AHR (Augmented Haptic Rehabilitation). The AHR is capable of delivering therapeutic forces (in an assist-as-needed manner) while keeping the hand tremor under control and avoiding unsafe amplification of tremor energy. This architecture makes it possible for patients living with pathological hand tremor to take advantage of robotic rehabilitation. The design of the proposed AHR architecture is motivated by recent evidence showing the impact of multi-modal rehabilitation for enhancing motor control in

patients living with pathological hand tremor. The proposed AHR architecture was implemented using an upper-limb rehabilitation robot from Quanser Inc. (Markham, Ontario, Canada), and its performance was evaluated experimentally. It was shown that using the proposed AHR architecture, assistance can be delivered to the voluntary component of the hand motion (in an adaptive manner) while the system can control involuntary hand tremors. Future work in this study is to longitudinally analyze the improvement that can be achieved by the use of the proposed AHR system on a group of PD and ET patients.

REFERENCES

[1] United Nations, Department of International Economic and Social Affairs, Population Division, *World Population Ageing*, 2013.

[2] J. Shahed and J. Jankovic, "Exploring the relationship between essential tremor and parkinson's disease," *Parkinsonism & Related Disorders*, vol. 13, no. 2, pp. 67–76, 2007.

[3] E. D. Louis and J. P. G. Vonsattel, "The emerging neuropathology of essential tremor," *Movement Disorders*, vol. 23, no. 2, pp. 174–182, 2008.

[4] K. Wirdefeldt, H.-O. Adami, P. Cole, D. Trichopoulos, and J. Mandel, "Epidemiology and etiology of parkinsons disease: a review of the evidence," *European Journal of Epidemiology*, vol. 26, no. 1, pp. 1–58, 2011.

[5] E. Rocon, M. Manto, J. Pons, S. Camut, and J. M. Belda, "Mechanical suppression of essential tremor," *The Cerebellum*, vol. 6, no. 1, pp. 73–78, 2007.

[6] E. Rocon, J. Belda-Lois, A. Ruiz, M. Manto, J. C. Moreno, and J. Pons, "Design and validation of a rehabilitation robotic exoskeleton for tremor assessment and suppression," *IEEE Transactions on Neural Systems and Rehabilitation Engineering*, vol. 15, no. 3, pp. 367–378, 2007.

[7] L. P. Maneski, N. Jorgovanović, V. Ilić, S. Došen, T. Keller, M. B. Popović *et al.*, "Electrical stimulation for the suppression of pathological tremor," *Medical & Biological Engineering & Computing*, vol. 49, no. 10, pp. 1187–1193, 2011.

[8] R. J. OConnor and M. U. Kini, "Non-pharmacological and non-surgical interventions for tremor: a systematic review," *Parkinsonism & Related Disorders*, vol. 17, no. 7, pp. 509–515, 2011.

[9] K. Kiguchi and Y. Hayashi, "An emg-based control for an upper-limb power-assist exoskeleton robot," *IEEE Transactions on Systems, Man, and Cybernetics, Part B: Cybernetics*, vol. 42, no. 4, pp. 1064–1071, 2012.

[10] C. N. Riviere, S. G. Reich, and N. V. Thakor, "Adaptive fourier modeling for quantification of tremor1," *Journal of Neuroscience Methods*, vol. 74, no. 1, pp. 77–87, 1997.

[11] C. N. Riviere, R. S. Rader, and N. V. Thakor, "Adaptive cancelling of physiological tremor for improved precision in microsurgery," *IEEE Transactions on Biomedical Engineering*, vol. 45, no. 7, pp. 839–846, 1998.

[12] K. C. Veluvolu, U.-X. Tan, W. T. Latt, C. Shee, and W. T. Ang, "Bandlimited multiple fourier linear combiner for real-time tremor compensation," in *IEEE Annual Engineering in Medicine and Biology Society (EMBS) Conference*, 2007, pp. 2847–2850.

[13] K. Veluvolu and W. Ang, "Estimation and filtering of physiological tremor for real-time compensation in surgical robotics applications," *The International Journal of Medical Robotics and Computer Assisted Surgery*, vol. 6, no. 3, pp. 334–342, 2010.

[14] K. Veluvolu, W. Latt, and W. Ang, "Double adaptive bandlimited multiple fourier linear combiner for real-time estimation/filtering of physiological tremor," *Biomedical Signal Processing and Control*, vol. 5, no. 1, pp. 37–44, 2010.

[15] S. Wang, Y. Gao, J. Zhao, and H. Cai, "Adaptive sliding bandlimited multiple fourier linear combiner for estimation of pathological tremor," *Biomedical Signal Processing and Control*, vol. 10, pp. 260–274, 2014.

[16] K. C. Veluvolu and W. T. Ang, "Estimation of physiological tremor from accelerometers for real-time applications," *Sensors*, vol. 11, no. 3, pp. 3020–3036, 2011.

[17] S. Tatinati, K. C. Veluvolu, and W. T. Ang, "Multistep prediction of physiological tremor based on machine learning for robotics assisted microsurgery," *IEEE Transactions on Cybernetics*, vol. 45, no. 2, pp. 328–339, 2015.

[18] K. C. Veluvolu, S. Tatinati, S.-M. Hong, and W. T. Ang, "Multistep prediction of physiological tremor for surgical robotics applications," *IEEE Transactions on Biomedical Engineering*, vol. 60, no. 11, pp. 3074–3082, 2013.

[19] H. I. Krebs, B. T. Volpe, M. Aisen, W. Hening, S. Adamovich, H. Poizner *et al.*, "Robotic applications in neuromotor rehabilitation," *Robotica*, vol. 21, no. 01, pp. 3–11, 2003.

[20] H. Krebs, N. Hogan, W. Hening, S. Adamovich, and H. Poizner, "Procedural motor learning in parkinson's disease," *Experimental Brain Research*, vol. 141, no. 4, pp. 425–437, 2001.

[21] S. Levy-Tzedek, H. I. Krebs, J. Shils, D. Apetauerova, and J. Arle, "Parkinson's disease: a motor control study using a wrist robot," *Advanced Robotics*, vol. 21, no. 10, pp. 1201–1213, 2007.

[22] G. M. Petzinger, B. E. Fisher, S. McEwen, J. A. Beeler, J. P. Walsh, and M. W. Jakowec, "Exercise-enhanced neuroplasticity targeting motor and cognitive circuitry in parkinson's disease," *The Lancet Neurology*, vol. 12, no. 7, pp. 716–726, 2013.

[23] N. E. Allen, N. Moloney, V. van Vliet, and C. G. Canning, "The rationale for exercise in the management of pain in parkinson's disease," *Journal of Parkinson's Disease*, 2015.

[24] E. E. van Wegen, M. A. Hirsch, M. Huiskamp, and G. Kwakkel, "Harnessing cueing training for neuroplasticity in parkinson disease," *Topics in Geriatric Rehabilitation*, vol. 30, no. 1, pp. 46–57, 2014.

[25] G. Frazzitta, R. Maestri, G. Bertotti, G. Riboldazzi, N. Boveri, M. Perini *et al.*, "Intensive rehabilitation treatment in early parkinsons disease a randomized pilot study with a 2-year follow-up," *Neurorehab. and Neural Repair*, vol. 29, no. 2, pp. 123–131, 2015.

[26] G. Sequeira, J. W. Keogh, and J. J. Kavanagh, "Resistance training can improve fine manual dexterity in essential tremor patients: a preliminary study," *Archives of physical medicine and rehabilitation*, vol. 93, no. 8, pp. 1466–1468, 2012.

[27] F. Budini, M. M. Lowery, M. Hutchinson, D. Bradley, L. Conroy, and G. De Vito, "Dexterity training improves manual precision in patients affected by essential tremor," *Archives of physical medicine and rehabilitation*, vol. 95, no. 4, pp. 705–710, 2014.

[28] J. J. Kavanagh, J. Wedderburn-Bisshop, and J. W. Keogh, "Resistance training reduces force tremor and improves manual dexterity in older individuals with essential tremor," *Journal of Motor Behavior*, no. ahead-of-print, pp. 1–11, 2015.

[29] S. F. Atashzar, A. Saxena, M. Shahbazi, and R. V. Patel, "Involuntary movement during haptics-enabled robotic rehabilitation: Analysis and control design," in *IEEE/RSJ International Conference on Intelligent Robots and Systems (IROS)*. IEEE, 2014, pp. 3561–3566.

[30] Y. Wang and K. Veluvolu, "Time-frequency decomposition of band-limited signals with bmflc and kalman filter," in *2012 7th IEEE Conference on Industrial Electronics and Applications (ICIEA)*. IEEE, 2012, pp. 582–587.

[31] S. Tatinati, K. C. Veluvolu, S.-M. Hong, W. T. Latt, and W. T. Ang, "Physiological tremor estimation with autoregressive (ar) model and kalman filter for robotics applications," *IEEE Sensors Journal*, vol. 13, no. 12, pp. 4977–4985, 2013.

[32] F. Wang and V. Balakrishnan, "Robust kalman filters for linear time-varying systems with stochastic parametric uncertainties," *IEEE Transactions on Signal Processing*, vol. 50, no. 4, pp. 803–813, 2002.

[33] K. Reif, S. Günther, E. Yaz, and R. Unbehauen, "Stochastic stability of the discrete-time extended kalman filter," *IEEE Transactions on Automatic Control*, vol. 44, no. 4, pp. 714–728, 1999.

[34] H. Taghirad, S. F. Atashzar, and M. Shahbazi, "Robust solution to three-dimensional pose estimation using composite extended kalman observer and kalman filter," *IET Computer Vision*, vol. 6, no. 2, pp. 140–152, 2012.

[35] B. Hannaford and J.-H. Ryu, "Time-domain passivity control of haptic interfaces," *IEEE Transactions on Robotics and Automation*, vol. 18, no. 1, pp. 1–10, 2002.

Seyed Farokh Atashzar (S'11) obtained his B.Sc. degree in Electrical Engineering/Control Systems from K. N. Toosi University of Technology, Tehran, Iran, in 2008 and his M.Sc. degree in Mechatronics from Amirkabir University of Technology, Tehran, Iran, in 2011. Farokh joined the Department of Electrical and Computer Engineering at Western University (UWO), London, Ontario, Canada, in 2011, to pursue his Ph.D. degree under the supervision of Professor Rajni Patel. His research work is being carried out at Canadian Surgical Technologies and Advanced Robotics (CSTAR). He also served as a visiting research scholar at the University of Alberta, AB, Canada, in 2014. During his Ph.D., He has received several awards including the prestigious Ontario Graduate Scholarship (OGS) in 2013 and NSERC CREATE program scholarship in Computer-Assisted Medical Intervention (CAMI) in 2011. His research areas include advanced haptic and telerobotic systems, rehabilitation and surgical robotics, mechatronics, vision-guided robot navigation, and robust nonlinear control theory.

Mahya Shahbazi (S'10) received the B.Sc. degree in electrical engineering from K. N. Toosi University of Technology, Tehran, Iran, in 2008, and the M.Sc. degree in mechatronics from Amirkabir University of Technology, Tehran, in 2011. She is currently working toward the Ph.D. degree in electrical and computer engineering at the University of Western Ontario, London, ON, Canada. She is a doctoral trainee in the NSERC CREATE program in Computer-Assisted Medical Interventions and a research assistant at Canadian Surgical Technologies and Advanced Robotics (CSTAR), London, ON. She has been a visiting research scholar at the University of Alberta, AB, Canada, and also among the very few international students at Western University granted the prestigious OGS (Ontario Graduate Scholarship) award in 2014. Her research interests include medical robotics focusing on applications in surgical training and rehabilitation; haptics and teleoperation; mechatronics; and control systems.

Olivia Samotus graduated from University of Ottawa in 2013, obtaining her Honours Bachelor of Science: Specialization in Biochemistry (CO-OP) through her work at the Ottawa Hospital Research Institute Cancer Centre and internationally conducted electrophysiology research at Technische Universitt Darmstadt in Germany. Olivia has continued to develop a keen interest in neuroscience and has joined Western University to pursue her Master's of Science degree in Neuroscience under the supervision of Dr. Mandar Jog. Olivia currently holds a MITACS industry funded scholarship for her clinical research focus on optimizing treatment of movement disorders using sensor kinematic technology.

Mahdi Tavakoli is an Associate Professor in the Department of Electrical and Computer Engineering, University of Alberta, Canada. He received his BSc and MSc degrees in Electrical Engineering from Ferdowsi University and K.N. Toosi University, Iran, in 1996 and 1999, respectively. He received his PhD degree in Electrical and Computer Engineering from the University of Western Ontario, Canada, in 2005. In 2006, he was a post-doctoral researcher at Canadian Surgical Technologies and Advanced Robotics (CSTAR), Canada. In 2007-2008, he was an NSERC Post-Doctoral Fellow at Harvard University, USA. Dr. Tavakolis research interests broadly involve the areas of robotics and systems control. Specifically, his research focuses on haptics and teleoperation control, medical robotics, and image-guided surgery. Dr. Tavakoli is the lead author of Haptics for Teleoperated Surgical Robotic Systems (World Scientific, 2008).

Mandar S. Jog (MD, FRCPC) is the Director of the National Parkinson Foundation Centre of Excellence in Parkinson Disease and Movement disorders program at London Health Sciences Centre and a Professor of Neurology at Western University, both in London, Ontario, Canada. He is also one of the Assistant Directors of the Lawson Health Research Institute. He trained in Neurology in Toronto and completed a fellowship in movement disorders with Dr. Anthony Lang. This was followed by a 4-year post-doctoral fellowship in computational neuroscience at the Massachusetts Institute of Technology (Boston, Massachusetts, Us) and a visiting professorship at Stanford Research Institute in California, US. With 4 patents and 6 provisional patents for innovative technology he is the co-founder of Medtrode Inc. and founder of ManJog Enterprises and MDDT Inc. Dr. Jog's research attempts to probe the structure and function of the basal ganglia and their role in movement disorders. His research projects on which he has published more than 150 peer-reviewed papers, over 230 abstracts and two books, focused on (a) technology for the assessment and treatment of movement disorders; (b) speech, gait, balance, posture and planning; (c) virtual reality based navigation in movement disorders; (d) high resolution MRI; (e) animal models and electrophysiology of the basal ganglia; (f) human intraoperative electrophysiological recording; (g) computational modelling of information processing in the brain. Dr. Jog was awarded the Deans Award for Excellence in Research (2012), Queens Diamond Jubilee award (2013) and has been awarded the 2014 Faculty Scholar Award for exemplary research, teaching and service, the 2014 Presidents Award for Innovation from the London Health Sciences Centres and the 2015 Strategic Research Fund Award from the Lawson Health Research Institute.

Rajni V. Patel (M'76, SM'80, F'92, LF'13) received the PhD degree in Electrical Engineering from the University of Cambridge, England, in 1973 and currently holds the position of Distinguished University Professor and Tier-1 Canada Research Chair in the Department of Electrical and Computer Engineering with cross appointments in the Department of Surgery and the Department of Clinical Neurological Sciences in the Schulich School Medicine and Dentistry at Western University, Ontario, Canada. Dr. Patel also serves as Director of Engineering for Canadian Surgical Technologies & Advanced Robotics (CSTAR). He is a Life Fellow of the IEEE, and a Fellow of the ASME, the Royal Society of Canada and the Canadian Academy of Engineering. He has served on the editorial boards of the IEEE Transactions on Robotics, the IEEE/ASME Transactions on Mechatronics, the IEEE Transactions on Automatic Control, and Automatica, and is currently on the Editorial Board of the International Journal of Medical Robotics and Computer Assisted Surgery and the Journal of Medical Robotics Research.